

Supplementary Information

From Phosphorus Nanorods/C to Yolk-Shell P@Hollow C for Potassium-Ion Batteries: High Capacity with Stable Cyclic Performance

Xingkang Huang,^{a,*} Xiaoyu Sui,^a Weixiao Ji,^a Yale Wang,^a Deyang Qu,^a and Junhong Chen^{a,b,c,*}

a. Department of Mechanical Engineering, University of Wisconsin-Milwaukee, 3200 North Cramer Street, Milwaukee, WI, 53211, USA. E-mail: xkhuang@uwm.edu

b. Current address: Pritzker School of Molecular Engineering, University of Chicago, 5640 South Ellis Avenue, Chicago, IL 60637, USA. E-mail: junhongchen@uchicago.edu

c. Current address: Argonne National Laboratory, 9700 South Cass Avenue, Argonne, IL 60439, USA. E-mail: junhongchen@anl.gov

EXPERIMENTAL

Hollow carbon (HC) was synthesized by a Chemical vapor decomposition (CVD) method using acetylene as a carbon source. Calcium carbonate nano-powers (Great Wall Mineral, China) were loaded in a combustion boat, which was heated up to 620 °C under Ar flow prior to CVD growth of C layer with a flow rate of 50 mL min⁻¹. After deposition of carbon for 10 min, the acetylene gas was switched to Ar flow to protect the C from oxidation during cooling down to room temperatures. The resulting powers were washed by dilute hydrochloric acid to remove calcium carbonate template and were further rinsed using deionized (DI) water and isopropanol. The as-obtained HC was dried at 120 °C under vacuum after purging the oven chamber three times using Ar.

The red P was purified using boiling DI water and stored in the glovebox prior to use. P and the HC were loaded into a glass tube and sealed prior to being heated at 550 °C for 2 h, cooled down to 260 °C at 1 °C min⁻¹ and maintained at 260 °C for 24 h to convert white P to red P. The resulting P/HC was washed by carbon disulfide to remove the possibly existing white P residual and dried under vacuum.

The morphologies of the as-prepared samples were characterized by scanning electron microscopy (SEM) and energy-dispersive X-ray spectroscopy (EDS), performed on a Hitachi S-4800 SEM machine equipped with a Bruker EDS detector. Transmission electron microscopy (TEM) was carried out on a Hitachi H-9000-NAR machine operating at an acceleration voltage of 300 kV. Powder X-ray diffraction (XRD) was performed on a Bruker D8 DISCOVER diffractometer with Cu K α radiation. The surface area measurements were carried out by Brunauer, Emmett, and Teller (BET) N₂ adsorption/desorption on a Micromeritics ASAP 2020. Pore size was analyzed based on a quenched solid density functional theory (QSDFT) kernel applied to the adsorption branch using a slit pore model. X-ray photoelectron spectroscopy (XPS) spectra of samples were obtained using a PerkinElmer PHI 5440 ESCA spectrometer with monochromatic Mg K α radiation as the X-ray source. Thermogravimetric analysis (TGA) was carried out under Ar flow (50 mL min⁻¹) at a heating rate of 5 °C min⁻¹ on an SDT 2660 Simultaneous DSC-TGA instrument.

The charge/discharge performance was characterized by using 2032-type coin cells that were assembled in an argon-filled glove box, with oxygen and moisture content below 1 ppm. Electrodes were prepared by mixing the as-prepared materials as the active material, sodium carboxymethyl cellulose, styrene-butadiene rubber, and carbon black as a conductor with a weight ratio of 80:5:5:10 to form a slurry. The resulting slurries were coated onto a Cu foil current collector using the doctor blade method, which was cut into disks (1.1 cm in diameter) after drying and pressing. The typical electrode material loadings of ca. 1-1.2 mg cm⁻². The electrolyte was 2.4 M Potassium bis(fluorosulfonyl)imide (KFSI) dissolved in ethylene carbonate/ethyl methyl carbonate (1:1, v/v).

The coin cells were tested on a LAND battery tester with a cut-off voltage range between 0.01 and

3 V. The current densities and capacities were calculated based on the total mass of P/HC composites loaded on the electrodes. Note that the potassiation behavior was defined as “charge” because the P is an anode material. Cyclic voltammetry (CV) and electrochemical impedance spectroscopy (EIS) of the as-prepared anode were measured on a PARSTAT 4000 electrochemical station using a three-electrode cell, with the P/HC composite electrode as the working electrode, a potassium disk as the counter electrode, and a potassium arc as the reference electrode because of unable to punch out potassium ring. CV was carried out at a scanning rate of 0.05 mV s^{-1} while EIS was tested between 10,000-0.01 Hz with an amplitude of 10 mV.

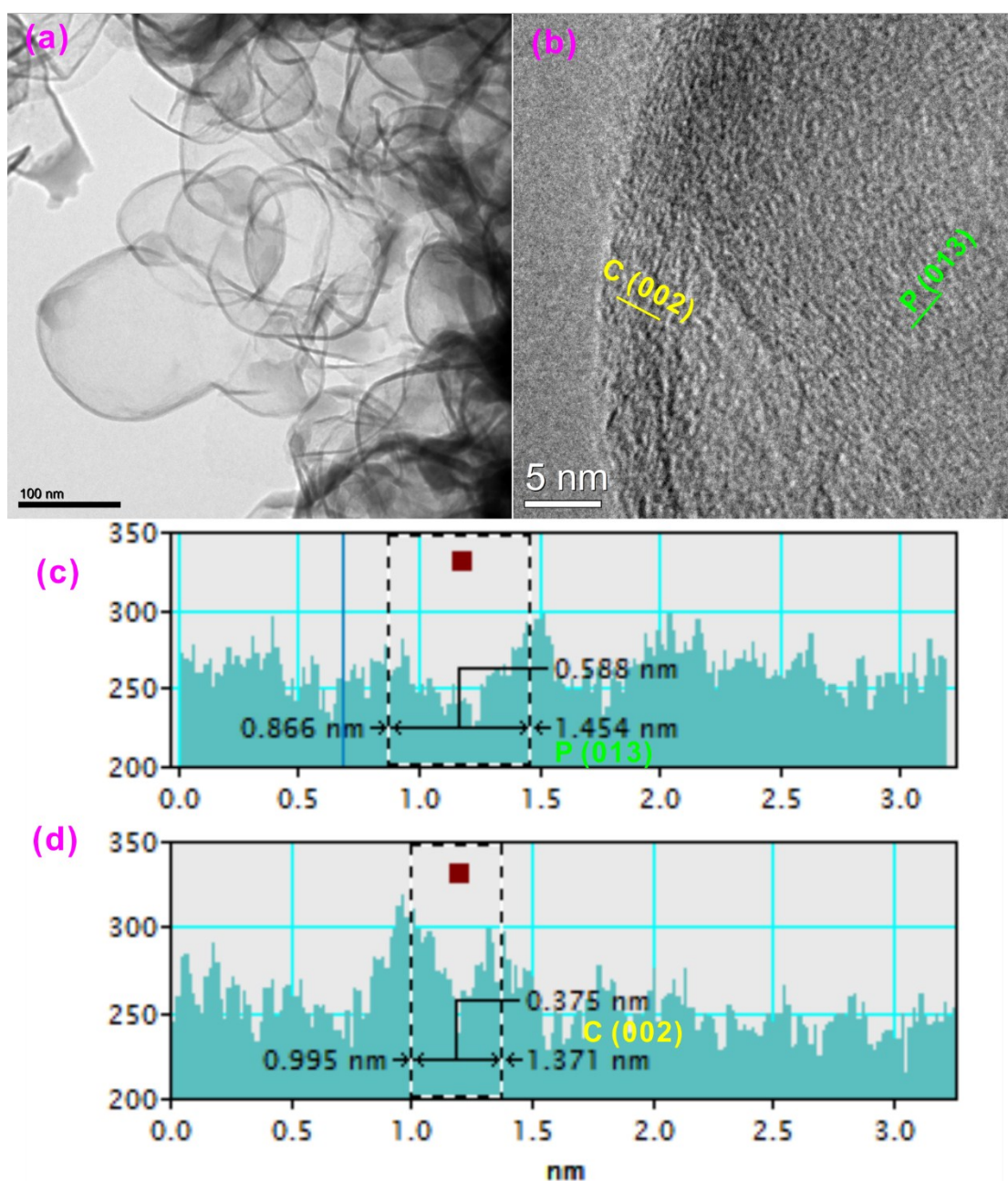


Figure S1. TEM analysis of the P@HC: (a) TEM images, (b) HRTEM image, and (c,d) profiles corresponding to the lattices marked with green and yellow lines, respectively, in b.

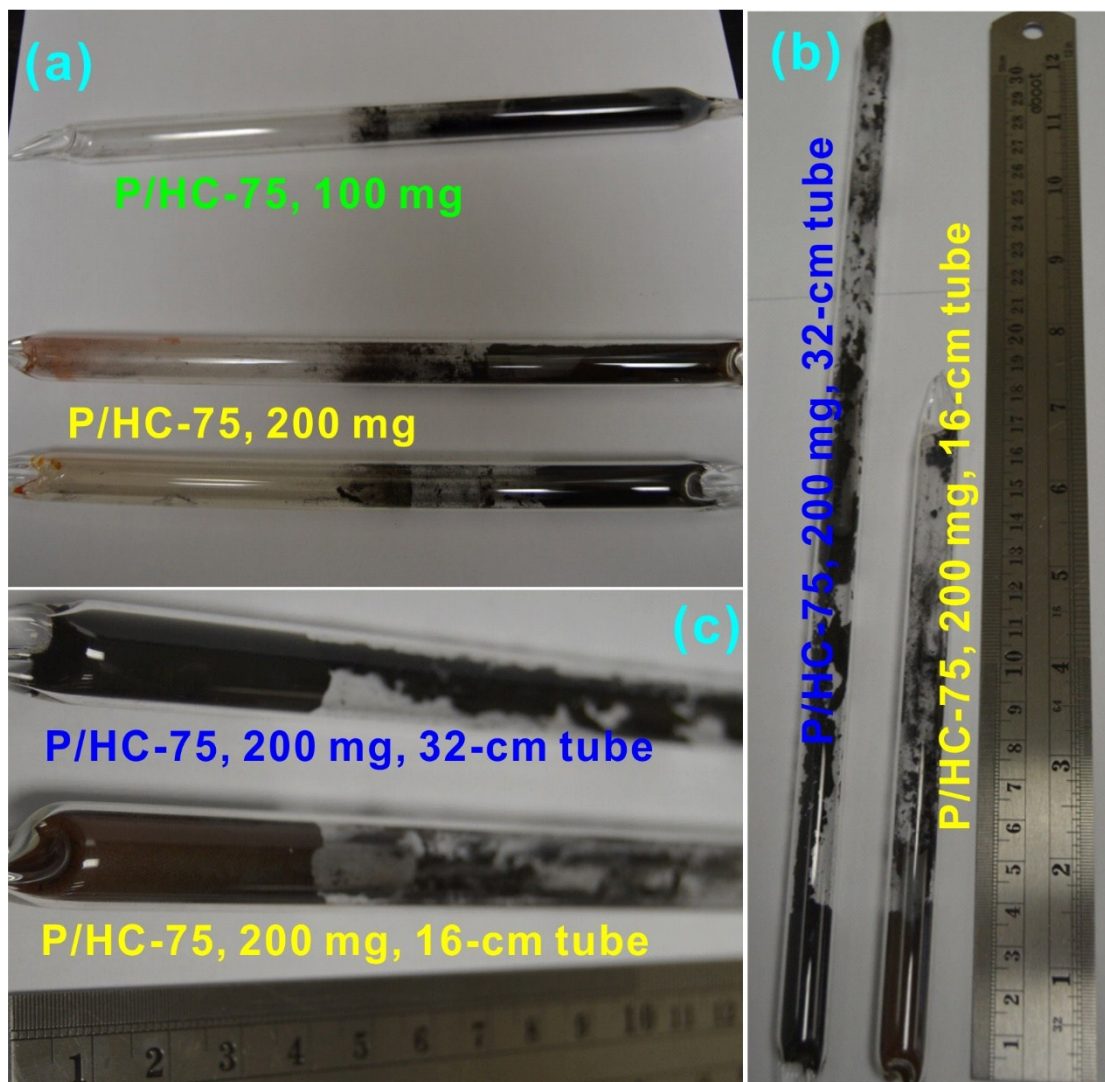


Figure S2. Optical photos of P/HC with the P content of 75 wt., prepared at various conditions: (a) with the same tube length but different mass loading in the tubes, (b,c) with the same P/C mass loading but different tube length.

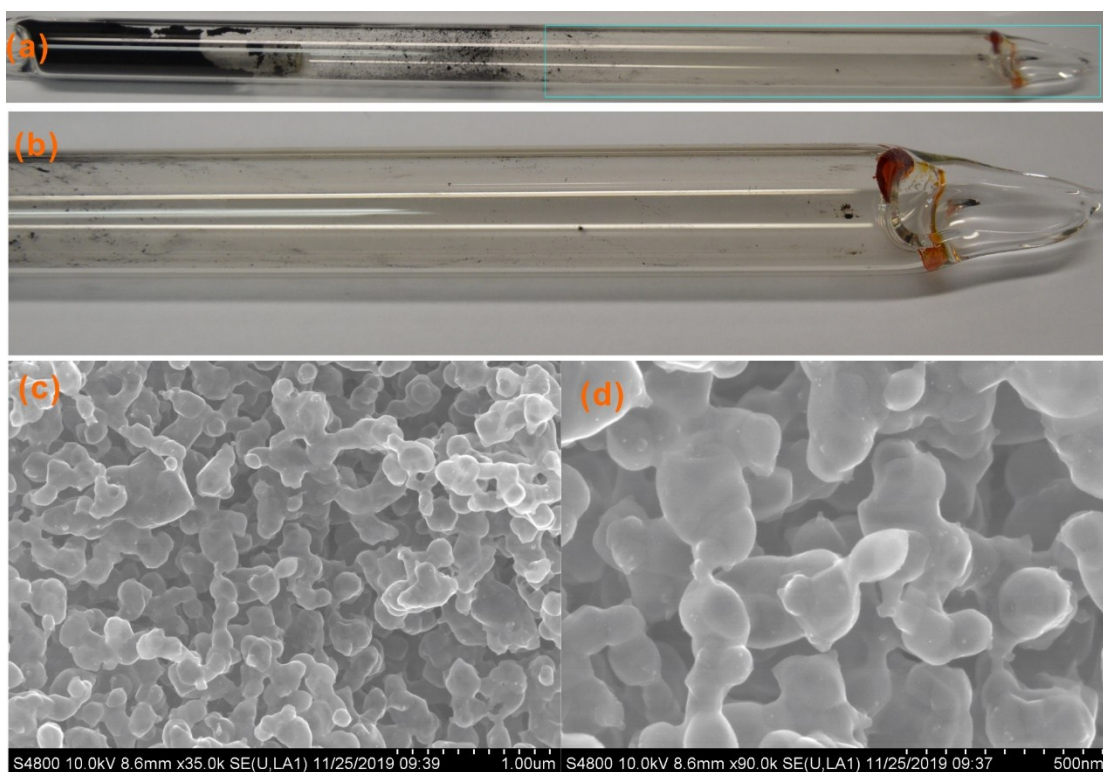


Figure S3. (a,b) Optical photograph of PNF/C with 80 wt. of P prepared in a 16-cm tube with 10 mg HC and 40 mg P. some red phosphorus was observed deposited on the right side (Figure b). (c,d) SEM image of the PNF/C with the low mass loading (50 mg).

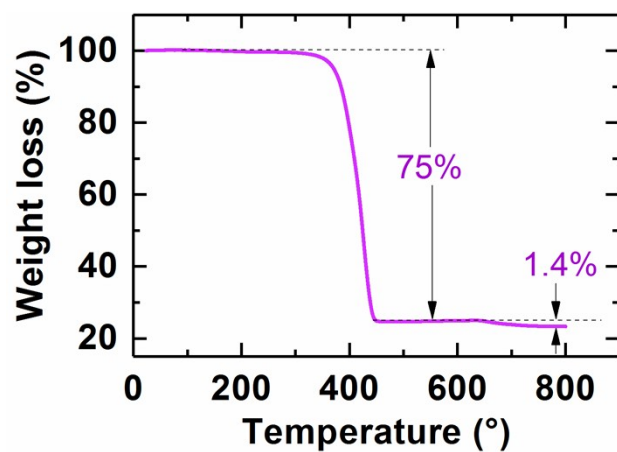


Figure S4. TGA curve of P@HC. The mass loss between 300-500 °C was 75 wt.%, which equals the P loading in the P@HC. An extra mass loss of 1.4 wt.% was observed at approximately 700 °C, which is uncertain at this stage, but could be related to the loss of oxygen containing groups from carbon surface.

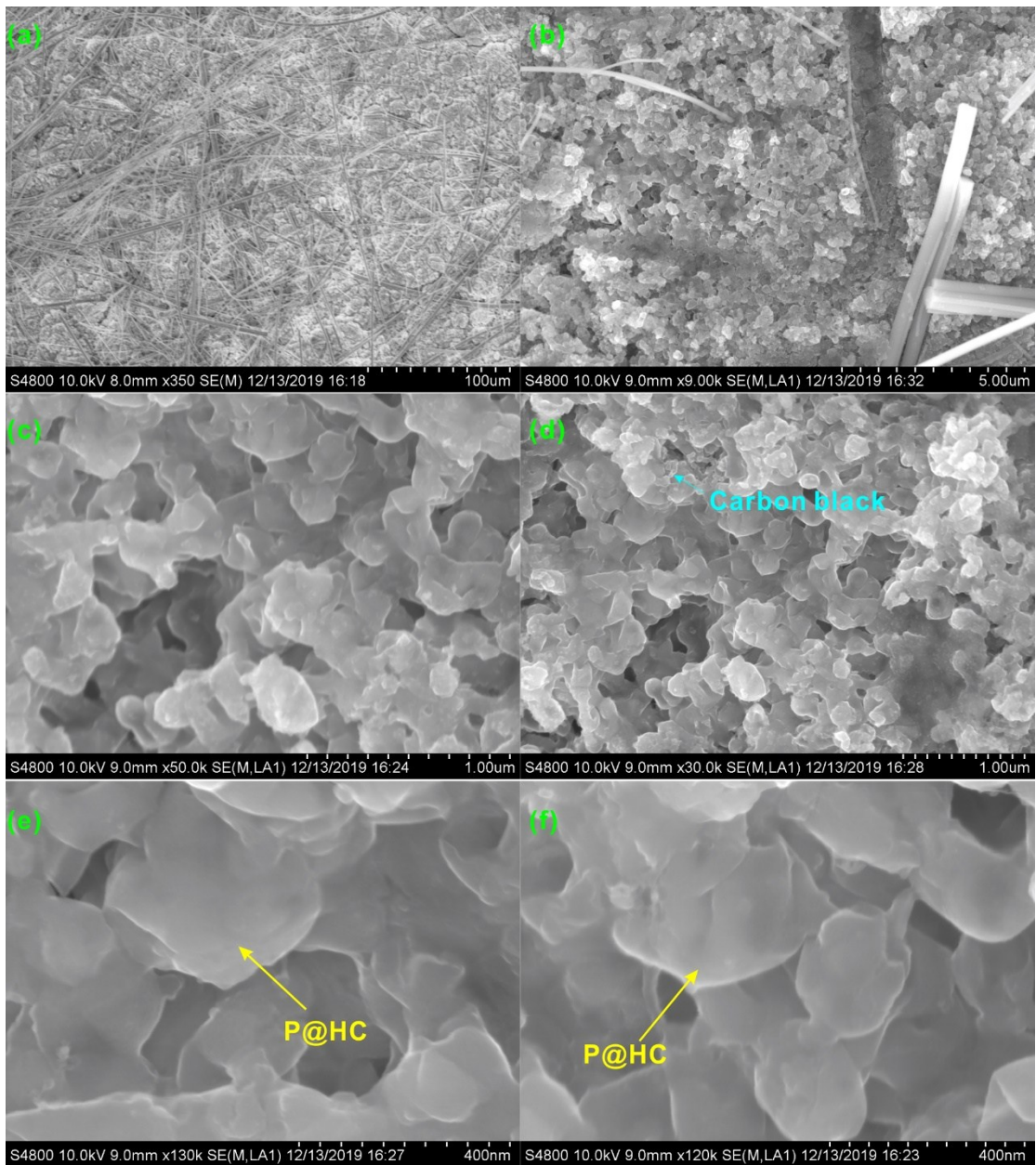


Figure S5 SEM images of the P@HC electrode after cycling. No significantly large cracks were observed on the electrode at various magnifications. Many glass fibers were observed on the surface of the electrode (Figure a,b), which could not be removed even washing many times using DMC, since some of them were imbedded in the surface of the electrode (Figure b). The sphere-like shape of the HC was well maintained after cycling and the P core can be observed encapsulated in the HC without cracking the carbon shells.

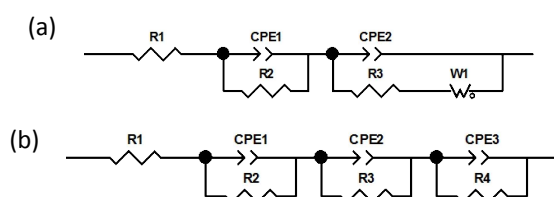


Figure S6. (a) Two-time constant and (b) three-time constant equivalent circuits for fitting the impedance results.

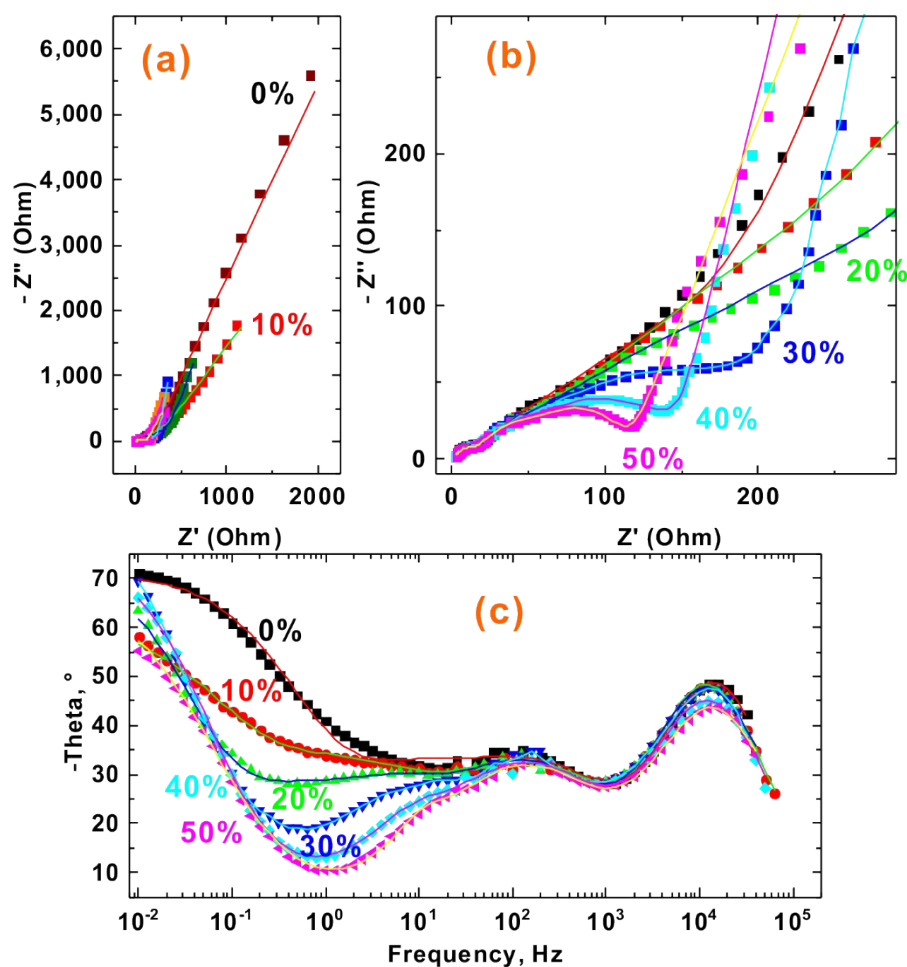


Figure S7. (a, b) Nyquist plots and (c) Bode plots of the P@HC at various states of charge, in which the fitting results (solid lines) were displayed with colors that are different from the corresponding experimental data on purpose to observe clearly how the fitting results match the experimental data. The impedance at 0% was fitted using a two-time constant equivalent circuit (Figure S6a), which led to clear deviation at the medium frequency zone (1-100 Hz, Figure S7c); other results were fitted using a three-time constant equivalent circuit (Figure S6b).

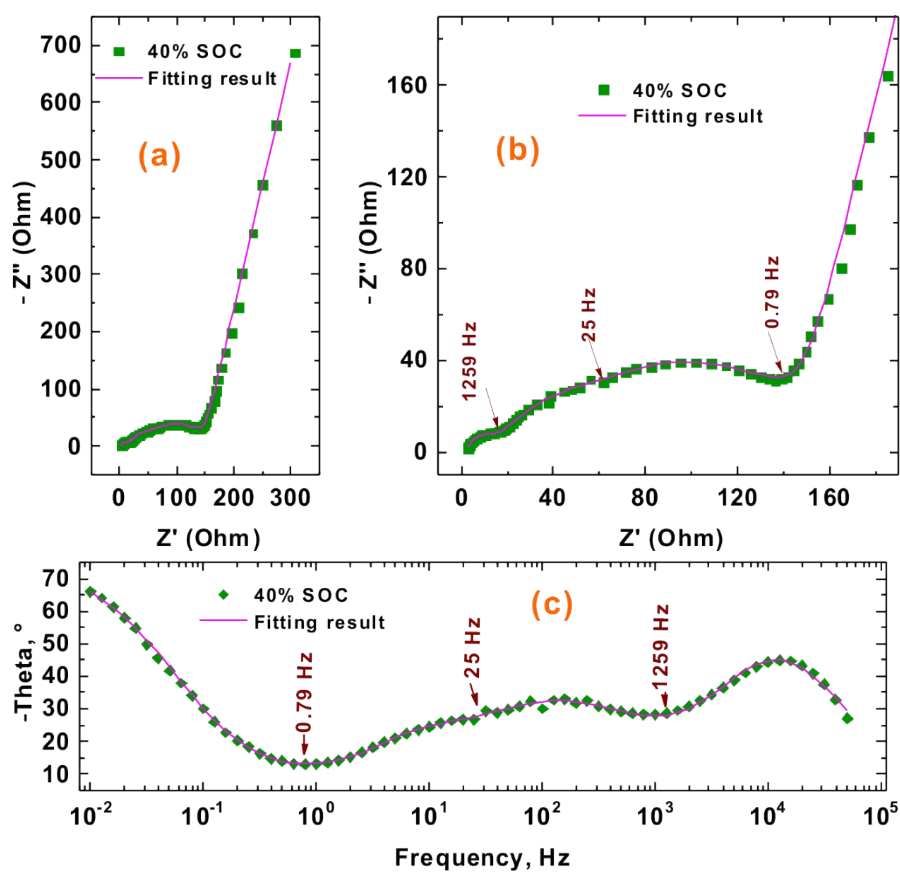


Figure S8. (a,b) Nyquist plots and (c) Bode plot of the P@HC electrode at 40% SOC.

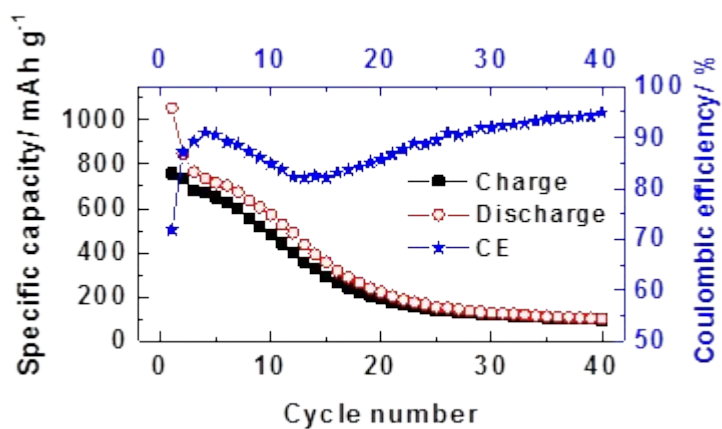


Figure S9. Cyclic performance of the PNR/C.

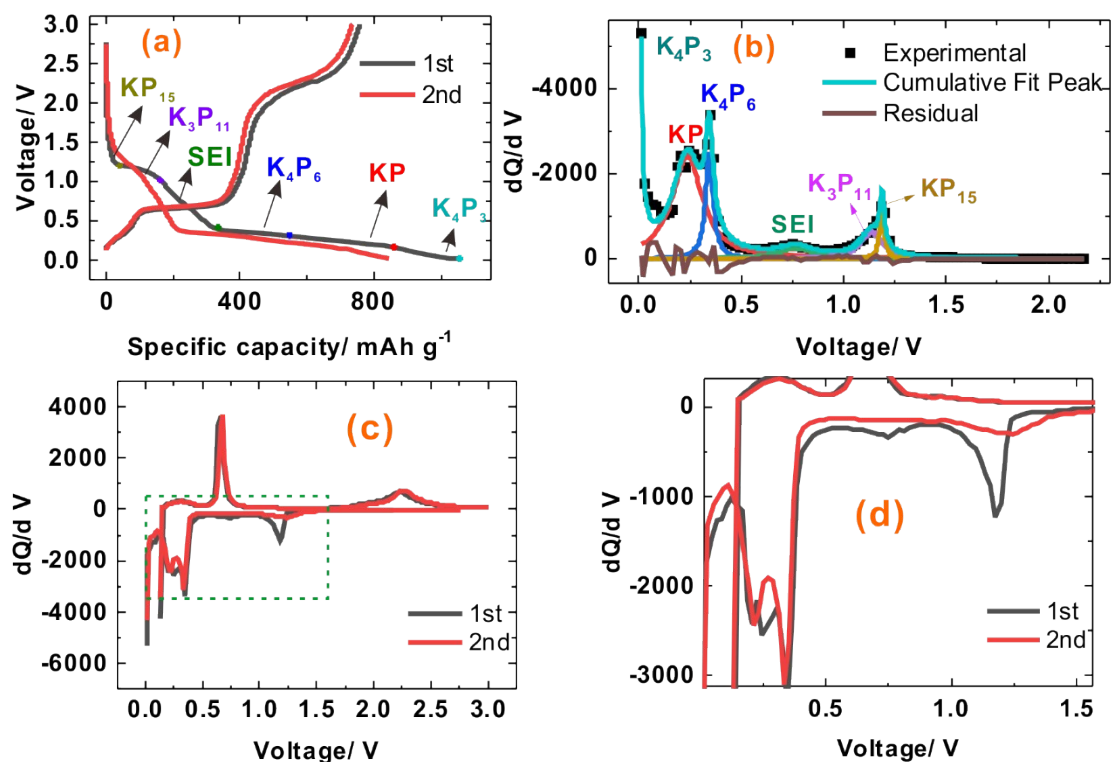


Figure S10. (a) Charge/discharge curves of PNR/C, (b) its dQ/dV plot for the first charge process, in which fitting results are shown in Table S4, and (c,d) comparison of the dQ/dV plots between the first and the second cycles.

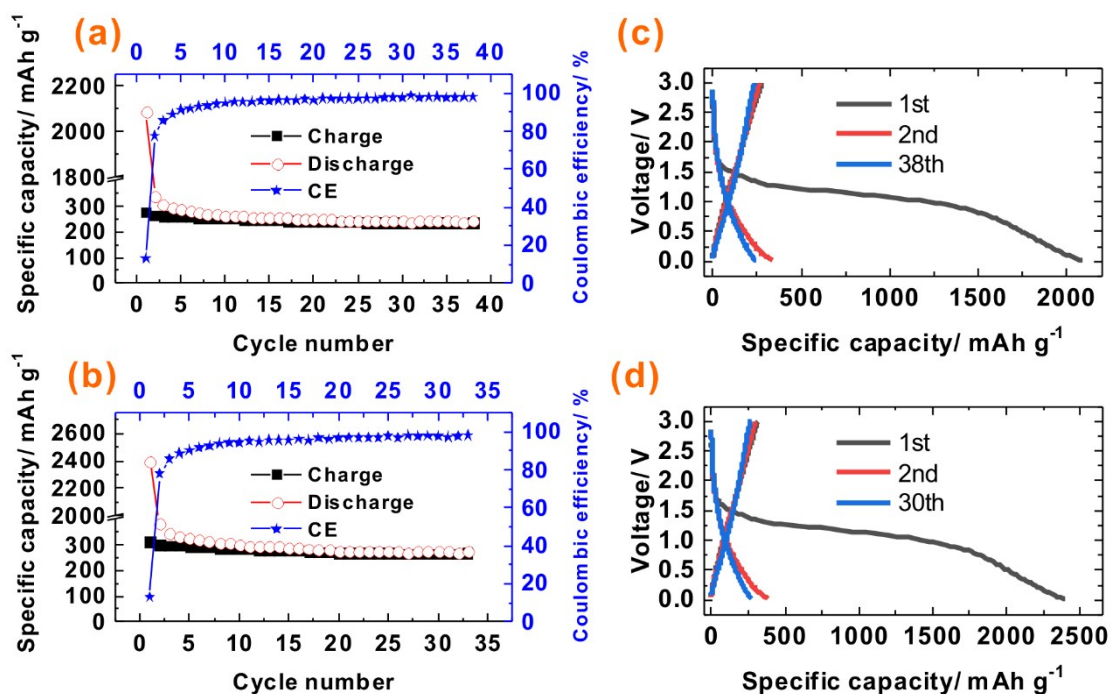


Figure S11. (a,b) Cyclic performance of two coin cell with the HC anode at 50 mA g^{-1} , and their corresponding charge/discharge curves are shown in (c) and (d), respectively. Because of the very low density of the HC, the mass loading on the electrode was typically $0.45\text{-}0.55 \text{ mg cm}^{-2}$, although

a doctor blade with a 8-mil gage was applied (i.e., 203 μm thickness for the wet coated slurry). No carbon black was added into the slurry to exclude the capacity contribution from carbon black. 20 wt.% of binder was required to help to improve the coating quality of the HC due to the large volume of the HC. The average reversible capacity of the HC at 50 mA g^{-1} was approximately 270 mAh g^{-1} , which showed slight decay in the initial 10 cycles and then stably remained at approximately 250 mAh g^{-1} .

Table S1. The effect of P vapor concentration on the morphology of P/C composite.

Composite, mg	P content,	C amount, mg	P amount, mg	Tube length, cm	P vapor pressure, Pa	P vapor concentration, mol/cm ³ *	Morphology
100	80	20	80	16	293.0	5.14E-05	Nanorods
100	75	25	75	16	274.7	4.82E-05	Yolk/shell
200	75	50	150	16	549.4	9.63E-05	Nanorods
200	75	50	150	32	274.7	4.82E-05	Yolk/shell
50	80	10	40	16	146.5	2.57E-05	Yolk/shell

* The pressure was calculated at 416 °C, which is the sublimation temperature of red P.

Table S2. Fitting results for the impedance at 40% SOC.

SOC%	R1(+)	R1(Err)	CPE1- T(+) ×10 ⁻⁶	CPE1- T(Err%)	CPE1- P(+)	CPE1- P(Err%)	R2(+)	R2(Err%)	CPE2- T(+) ×10 ⁻⁴	CPE2- T(Err%)	CPE2- P(+)	CPE2- P(Err%)	R3(+)	R3(Err%)	CPE3- T(+) ×10 ⁻⁴	CPE3- T(Err%)	CPE3- P(+)	CPE3- P(Err%)	R4(+)	R4(Err%)	W1- R(+)	W1- R(Err%)	W1- T(+)	W1- T(Err%)	W1- P(+)	W1- P(Err%)
0	2.2	2.1	3.8	10.3	1.0	1.2	13.0	3.8	3.2	7.4	0.7	2.3	94.8	14.2	8.0	26.9	0.8	12.2	393.7	144.7	0.2	7.7E+05	2.3E-05	9.6E+05	0.40	6.98
10	2.3	1.4	3.5	11.2	1.0	1.3	11.4	4.8	3.9	12.1	0.7	6.0	57.0	31.8	12	20.8	0.7	15.1	425.1	106.4	0.1	1.1E+06	6.9E-06	1.5E+06	0.35	6.97
20	2.3	1.2	4.0	9.7	1.0	1.1	12.4	3.7	2.3	10.1	0.7	2.3	78.8	4.4	1.1	11.9	1.3	1.6	8E-7	4.4E+07	698.7	2.4	8.1	3.5	0.42	0.78
30	2.2	1.9	5.2	11.5	0.9	1.4	12.3	5.3	2.5	14.1	0.7	3.4	74.1	13.3	3.5	16.7	1.1	7.8	50.2	26.3	244.3	4.8	3.5	6.4	0.44	0.44
40	2.4	1.8	5.5	14.3	0.9	1.8	11.4	7.1	2.8	19.3	0.7	4.6	79.0	19.8	3.6	31.4	1.1	14.8	27.5	61.2	84.2	12.4	1.4	15.8	0.43	0.50
50	2.4	1.9	8.1	12.8	0.9	1.6	12.3	6.1	2.4	26.9	0.7	4.3	65.9	24.6	4.7	611.1	1.1	110.4	34.0	1.3E+03	6.0	2.1E+04	4.9E-02	2.8E+04	0.38	2.25
60	1.8	22.7	1.9E-05	35.3	0.8	5.2	14.6	11.9	2.2	25.2	0.8	6.1	59.7	25.2	4.2	218.6	1.1	40.3	29.7	1.0E+03	2.8	3.2E+04	1.4E-02	4.5E+04	0.36	1.16
70	1.7	19.6	2.0E-05	29.2	0.8	4.3	14.6	10.1	2.4	21.9	0.7	5.4	58.4	23.5	4.7	135.2	1.1	27.7	26.7	1.5E+03	1.2	1.0E+05	3.3E-03	1.6E+05	0.32	0.99
80	1.6	16.4	2.1E-05	22.1	0.8	3.3	14.7	7.2	2.6	14.7	0.7	3.6	64.3	14.7	6.8	123.4	1.1	22.8	24.0	1.4E+03	0.6	1.6E+05	4.5E-03	2.3E+05	0.35	0.81
90	1.6	16.4	21	22.1	0.8	3.3	14.7	7.2	2.6	14.7	0.7	3.6	64.3	14.7	6.8	123.4	1.1	22.8	24.0	1.4E+03	0.6	1.6E+05	4.5E-03	2.3E+05	0.35	0.81
100	1.6	22.7	23	29.4	0.8	4.4	14.9	10.0	2.3	22.3	0.8	5.5	45.3	19.0	4.9	139.0	1.0	22.7	26.1	1.1E+03	0.4	2.0E+05	5.8E-03	2.7E+05	0.37	0.71

Due to the highly over-lapped time constants, it was very difficult to fit the impedance results. The use of a two-time constant led to obvious deviation of the fitting results from the experimental data (Figure S7, 0% SOC). In contrast, the use of a three-time constant equivalent circuit resulted in apparently well fitted data; however, the fitting errors of some parameters related with R4 and W1-R were much higher than 100%, except the cases of 30 and 40% SOCs. Considering that the impedance changes were relatively small at the SOCs between 40 and 90%, The resistances of the electrode can be reflected by the SOC of 40%, showing 2.4, 11.4, 79, 27.5, and 84.2 Ohm for R1, R2, R3, R4 and W1-R, respectively. R1 is Ohmic resistance and R2 represents the SEI layer resistance. R3 and R4 could be the charge transfer resistances on the HC and the P in the P@HC, respectively; however, further investigation is necessary for conformation.

Table S3. Crystal information of K-P alloys, capacity and volume change upon potassiation

Phase	Red P	KP ₁₅	K ₃ P ₁₁	α -K ₄ P ₆	β -K ₄ P ₆	KP	K ₄ P ₃	K ₃ P
Crystal system	Monoclinic	Triclini c	Orthorhombic	Orthorhombic	Orthorhombic	Orthorhombic	Orthorhombic	Hexagona l
Space group	<i>P2/c</i>	P-1	<i>Pnab</i>	<i>Fmmm</i>	<i>Fddd</i>	<i>P212121</i>	<i>Cmcm</i>	<i>P63/mmc</i>
Space group number	13	2	60	69	70	19	63	194
a (Å)	10.044	23.74	10.315	9.347	18.65	6.5	5.049	5.691
b (Å)	9.225	9.69	13.94	14.253	14.772	6.016	11.197	5.691
c (Å)	24.497	7.21	10.45	8.624	8.305	11.288	14.788	10.05
Alpha (°)	90	116.7	90	90	90	90	90	90
Beta (°)	118.3	97.5	90	90	90	90	90	90
Gamma (°)	90	90.0	90	90	90	90	90	120
Calculated density (g/cm ³)	2.16	2.28	2.02	1.98	1.99	2.11	1.98	1.75
Volume of cell (10 ⁶ pm ³)	1998.5	1465.8	1502.62	1148.91	2288.01	441.41	836.02	281.89
Z	84	4	4	4	8	8	4	2
Volume per P unit (10 ⁶ pm ³)	23.79	24.43	34.15	47.87	47.67	55.18	69.67	140.95
Volume change	N/A	2.7	43.5	101.2	100.4	131.9	192.9	492.5
Capacity, mAh g ⁻¹ *	N/A	57.7	236.0	576.9	576.9	865.3	1153.7	2514.7

*Note: the capacity is referred to the value upon potassiating P to the corresponding K-P alloy phase.

Table S4 Summary on fitting results in Figure S8b

Peak	Area	Percentage, %
KP15	49.7	4.5
K3P11	120.9	11.0
SEI	76.2	6.9
K4P6	167.3	15.2
KP	587.7	53.3
K4P3	99.9	9.1